NASA TECHNICAL NOTE

NASA TN D-3249

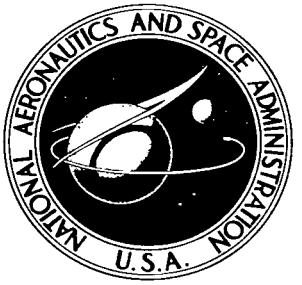

NASA TN D-3249

SIMULATOR FOR STATIC LIQUID CONFIGURATION IN PROPELLANT TANKS SUBJECT TO REDUCED GRAVITY

by William A. Olsen

Lewis Research Center
Cleveland, Ohio

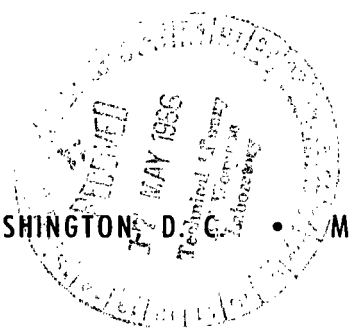

NATIONAL AERONAUTICS AND SPACE ADMINISTRATION • WASHINGTON, D. C. • MAY 1966

SIMULATOR FOR STATIC LIQUID CONFIGURATION IN PROPELLANT TANKS SUBJECT TO REDUCED GRAVITY

By William A. Olsen

Lewis Research Center
Cleveland, Ohio

NATIONAL AERONAUTICS AND SPACE ADMINISTRATION

For sale by the Clearinghouse for Federal Scientific and Technical Information
Springfield, Virginia 22151 – Price $2.00

SIMULATOR FOR STATIC LIQUID CONFIGURATION IN PROPELLANT TANKS SUBJECT TO REDUCED GRAVITY

by William A. Olsen

Lewis Research Center

SUMMARY

A simple device has been investigated and constructed which can approximately simulate (show) the isothermal equilibrium liquid configuration in propellant tanks of various shapes and sizes that are subject to reduced gravity ranging from 1 to near "zero" gravity. Experimental results compare favorably with drop-tower results.

The simulator, an application of the "Hele-Shaw Cell," is basically composed of two parallel, closely spaced, flat glass plates that are separated by rubber gaskets, which are cut to form the two-dimensional tank boundary. A given amount of liquid is placed within these boundaries. The angle of the plates to the horizontal is varied to obtain various effective gravity fields. The basic principle of the simulator can be roughly stated in the following manner: When two parallel, flat plates are closely spaced, the two-dimensional liquid shape in the plane of the plates is only affected by the gravity component and the tank boundaries in that plane. Thus, when the plates are perfectly horizontal, the liquid should assume the zero-gravity shape[1] for the particular two-dimensional tank boundaries and liquid used between the plates.

The design and operating criteria for the device that allow it to simulate the static liquid shape in two-dimensional tanks is obtained analytically and substantiated by experiments. The ability of the device to simulate three-dimensional tanks approximately is indicated experimentally. Sample photographs were taken of the equilibrium liquid configuration within the simulator for various gravity fields, tank sizes, and configurations.

INTRODUCTION

The NASA Lewis Research Center is conducting studies of the behavior of propellants in storage tanks while exposed to reduced gravity (ref. 1). This condition will be encountered by space vehicles during planetary orbital missions and during periods of coast on interplanetary space missions (ref. 2). A knowledge of the liquid configuration will be needed to solve problems related to effective tank venting, liquid transfer, orientation control of the vehicles,

[1]For a given tank and liquid, zero gravity is that gravity below which changes in gravity have a negligible effect on liquid configuration (i.e., Bond number $< 10^{-2}$).

and heat transfer (ref. 1).

Reduced gravity studies of the static liquid configuration in propellant tanks have been generally limited to specific analytical studies (refs. 3 and 4) and experiments (refs. 5 and 6). A device that quickly, simply, and inexpensively shows the approximate shape of a liquid in a tank subject to reduced gravity could greatly help the engineer and designer in this new field. Many different experimental methods have been used to obtain the reduced-gravity liquid configuration, such as drop towers, zero-gravity trajectories in aircraft, and a simulator using the same density but different surface tension liquids. In this investigation another approach was taken that involved a two-dimensional simulator to determine the approximate static liquid configuration within propellant tanks of varying shapes and sizes, which were subject to effective gravity fields from near zero gravity to 1 g.

This report describes this simulator and shows some of the results obtained. The simulator is composed of two parallel, closely spaced, flat glass plates, separated by rubber gaskets, which form the two-dimensional tank boundary. Liquid is placed within these boundaries. The angle of the plates to the horizontal is varied to obtain various effective gravity fields.

The idea of using two parallel glass plates for fluid studies is not new. Hele-Shaw (ref. 7) devised a similar arrangement to study two-dimensional potential flow around objects. Reference 8 later used this same method to simulate the stability of the interface between two different liquids as they flowed through a porous media. In this reference, it is suggested that the effect of gravity would disappear when the plates were horizontal.

The basis for the device in this application is derived and discussed. Some liquid configuration data are obtained for static situations.

ANALYTICAL BASIS FOR SIMULATION OF STATIC LIQUID SHAPE IN TANKS

In this section the design and operating conditions for a two-dimensional simulator of the static liquid shape in containers of various sizes subject to varying gravity fields will be derived. Theory for scaling simulator results to two- and three-dimensional containers of various sizes in various gravity fields will be discussed. The analysis that follows is basically an application of the type of analysis found in a number of references, for example references 3 and 4.

General Equations

Consider the energy of a fixed amount of liquid at rest, at constant temperature, with constant properties, in a simply formed tank where surface tension forces are significant. The shape of the liquid depends on the sum of the surface free energies and the potential energy of the liquid (ref. 9)

$$I = \sum_j \sigma_j \iint_{S_j} dS + g_o \rho_e \iiint_V nz \, dV \tag{1}$$

where

$$\rho_e = \rho_l - \rho_f$$

(All symbols are defined in appendix A.)

Expand equation (1) to include the surface free energies, respectively, of the liquid-solid (LS), solid-vapor (SV), and liquid-vapor (LV) interfaces of figure 1 to obtain

$$I = \sigma_{LS} \iint_{S_{LS}} dS + \sigma_{LV} \iint_{S_{LV}} dS + \sigma_{SV} \iint_{S_{SV}} dS + g_o \rho_e \iiint_V nz \, dV \tag{2}$$

The Dupre-Young equation (refs. 3 and 10), which relates the surface free energies per unit area to the contact angle[2] θ, is given as follows:

$$\sigma_{SV} - \sigma_{LS} = \sigma_{LV} \cos \theta \tag{3}$$

This equation strictly holds for $0^\circ < \theta < 180^\circ$, but it is assumed to be sufficiently accurate for this analysis even when $\theta = 0$.

Combine equation (2) with (3) to eliminate σ_{SV}. Then use equation (4), which breaks up the area of the container:

$$S_b = \iint_{S_{SV}} dS + \iint_{S_{LS}} dS \tag{4}$$

These substitutions result in

$$I = \sigma_{LV} \iint_{S_{LV}} dS + \sigma_{LV} \cos \theta \iint_{S_{SV}} dS + \sigma_{LS} S_b + g_o \rho_e \iiint_V nz \, dV \tag{5}$$

The configuration of a fixed amount of liquid in a tank is in stable equilibrium when this energy I is a minimum (ref. 12). Mathematically, this requires the variation of I to vanish (i.e., $\delta I = 0$) subject to the constraint of constant liquid volume. Performing the required variation operation upon equation (5)

[2]Available data from isothermal drop-tower experiments with no flow appear to indicate that the contact angle θ is a constant (ref. 11).

results in the following equation (eq. (6a)), which together with the constraint equation (eq. (7)) describes the liquid configuration in a given three-dimensional tank subject to a given gravity field

$$\delta I = \delta\left(\sigma_{LV} \iint_{S_{LV}} dS + \sigma_{LV} \cos\theta \iint_{S_{SV}} dS + \sigma_{LS} S_b + g_o \rho_e \iiint_V nz \, dV\right) = 0 \tag{6a}$$

and

$$\iiint_V dV = \text{constant} = V \tag{7}$$

It is possible at this point to simplify equation (6a) by eliminating the term $\sigma_{LS}S_b$ in an actual three-dimensional case, since it is a constant whose variation vanishes. This equation would then become

$$\delta\left(\sigma_{LV} \iint_{S_{LV}} dS + \sigma_{LV} \cos\theta \iint_{S_{SV}} dS + g_o \rho_e \iiint_V nz \, dV\right) = 0 \tag{6b}$$

However, this term must be kept for the subsequent analysis of the simulator because it may not be constant in that case.

Two-Dimensional Simulator

Equations (6a) and (7) will now be applied to the case of a two-dimensional tank model in a 1-g field which is bounded top and bottom by glass plates and around the edges by a two-dimensional model of a tank configuration (see fig. 2). In this situation, the surface energy is made up of the surface energies due to the two-dimensional model boundaries, the gas, and the top and bottom plates. Assume the surface tension properties are the same for edges and plates, then the equations governing the liquid configuration in this case are:

$$\delta\left[\sigma_{LV} \iint_{S_{LV}} dS + \sigma_{LV} \cos\theta \left(\iint_{S_{SVB}} dS + 2 \iint_{S_{SVP}} dS\right) + \sigma_{LS}(S_B + 2S_p) + g_o \rho_e \iiint_V nz \, dV\right] = 0 \tag{8}$$

where

$$S_b = S_B + 2S_p$$

and

$$\iint_{S_{SV}} dS = \iint_{S_{SVB}} + 2 \iint_{S_{SVP}} dS$$

Equation (8) is subject to the constraint

$$\iiint_{V} dV = \text{constant} = V \tag{9}$$

By analogy with the equations for a three-dimensional tank (eqs. (6a) and (7)) the equations for a two-dimensional tank would be

$$\delta\left(\sigma_{LV} \oint_{C_{LV}} ds + \sigma_{LV} \cos\theta \oint_{C_{SV}} ds + g_o\rho_e \oint\!\!\oint_{A} m\alpha \, dA\right) = 0 \tag{10}$$

and

$$\oint\!\!\oint_{A} dA = \text{constant} = A \tag{11}$$

The desired result is to have the simulator, a three-dimensional device, simulate the liquid shape in two-dimensional containers[3]. The question then is what assumptions are necessary to transform equations (8) and (9) into the form of euqations (10) and (11). These assumptions are given as follows:

(1) The plate spacing is small compared with the local characteristic width of the interface in the model. Usually this characteristic width is taken as the tank or capillary tube diameter.

(2) The plate spacing is less than the maximum spacing required for the liquid to contact both plates (see appendix B).

(3) The plates are flat and parallel (i.e., ξ = const.).

By these assumptions the liquid area $A(x, \alpha)$ (fig. 2), in the planes parallel to the plates is essentially unchanging in the direction normal to the plates (i.e., $\oint_C ds$ and $\oint\!\!\oint_A dA$ are not functions of β). Also, the element of volume dV can be taken as

$$dV = \xi \, dx \, d\alpha = \xi \, dA$$

Consider now the potential energy term of equation (8). Consider the

[3]A two-dimensional container is formed by infinite translation of the two-dimensional (plane) shape in the direction normal to the plane of the two-dimensional shape.

parallel plates to be inclined at an angle φ to the horizontal (see fig. 2). Then by using the preceding assumptions this term becomes

$$g_o\rho_e \iiint_V nz \, dV = g_o\rho_e \iiint_V n\alpha \sin\varphi \, dV = g_o\rho_e\xi \iint_A m\alpha \, dA$$

where $m = n \sin\varphi$, $z = \alpha \sin\varphi$, and $dV = \xi \, dx \, d\alpha$.

By the previous assumptions the integrals can each be integrated once in the β direction. Integrating each term of equations (8) and (9) results in

$$V = \text{constant} = \iiint_V dV = \xi \oint\oint_A dA$$

$$\oint\oint_A dA = \text{constant} = A$$

and similarly

$$\oint\oint_{A_{SV}} dA = A_{SV} = \text{constant}$$

$$\sigma_{LV} \iint_{S_{LV}} dS = \sigma_{LV} \oint_{C_{LV}} ds \int_0^{\xi} d\beta = \sigma_{LV}\xi \oint_{C_{LV}} ds$$

$$2(\sigma_{LV} \cos\theta) \iint_{S_{SVP}} dS = 2(\sigma_{LV} \cos\theta) \oint\oint_{A_{SV}} dA = 2(\sigma_{LV} \cos\theta)A_{SV} = \text{constant}$$

$$\sigma_{LV} \cos\theta \iint_{S_{SVB}} dS = \sigma_{LV} \cos\theta \oint_{C_{SV}} ds \int_0^{\xi} d\beta = \sigma_{LV} \cos\theta\xi \oint_{C_{SV}} ds$$

Finally,

$$\sigma_{LS}(S_B + 2S_p) = \sigma_{LS}(C_B\xi + 2A_T)$$

Substitute these relations into equations (8) and (9) and divide by ξ to obtain

$$\delta\left[\sigma_{LS}\left(C_B + \frac{2A_T}{\xi}\right) + 2\sigma_{LV} \cos\theta \frac{A_{SV}}{\xi} + \sigma_{LV} \oint_{C_{LV}} ds + \sigma_{LV} \cos\theta \oint_{C_{SV}} ds + g_o\rho_e \oint\oint_A m\alpha \, dA\right] = 0 \qquad (12)$$

The first two terms in equation (12), not involving integrals, are constants for a given case and the variation of a constant is zero; therefore, the equation can be reduced to

$$\delta\left(\sigma_{LV}\oint_{C_{LV}} ds + \sigma_{LV}\cos\theta\oint_{C_{SV}} ds + g_o\rho_e\iint_A m\alpha\, dA\right) = 0 \tag{13}$$

Equation (13), together with the constraint

$$\iint_A dA = \text{constant} = A \tag{14}$$

describes the shape of the liquid in the simulator. The equations describing the liquid shape in the simulator (eqs. (13) and (14)) and for a two-dimensional container (eqs. (10) and (11)) are of the same form if the assumptions used in the derivations are correct. By inspection, the two-dimensional liquid shape in the simulator is only affected by tank boundaries and surface energies in the plane of plates (α,x plane) with the magnitude of gravity taken as a component in that plane ($m = \sin\varphi$). The two-dimensional liquid shape is not affected by the plates. This result assumed the simulator to be designed with flat, parallel plates that are separated by a distance that is less than the maximum required for wetting and also required the characteristic interface dimension to be much greater than the plate spacing.

In order to make the liquid configuration in the simulator and in a larger two-dimensional container the same, the terms in the governing equations must be of the same magnitude, term by term (i.e., scaled), in addition to being of the same form. Scaling equations for magnitude is best handled by nondimensionalizing the variational equations describing the two-dimensional liquid configuration (eqs. (13) and (14)).

Equations describing the two-dimensional simulator and a two-dimensional container (eqs. (13) and (14)) are nondimensionalized by the following substitions

$$\alpha = \zeta\mathfrak{L}_s \qquad s_{LV} = c_{LV}\mathfrak{L}_s$$

$$A = a\mathfrak{L}_s^2 \qquad s_{SV} = c_{SV}\mathfrak{L}_s$$

$$\delta\left\{\oint_{c_{LV}} dc + \cos(\theta_s)\oint_{c_{SV}} dc + \left[\underbrace{mg_o\left(\frac{\rho_e}{\sigma_{LV}}\right)}_{B_s}\mathfrak{L}^2\right]_s\iint\zeta\, da\right\} = 0 \tag{15}$$

and

$$\iint_a da = a \tag{16}$$

where

$m = n$ for two-dimensional case

$m = \sin \varphi$ for simulator and $n = 1$

The nondimensionalization has been done so that the nondimensional variable integrals (lower-case script letters) vary within a unit order of magnitude, while the constant coefficients (nondimensional groups) in front of the integral signs, containing characteristic quantities, represent the magnitude of the term of which they are a part. It was assumed that adequate scaling could be achieved if the characteristic quantities were taken as a characteristic dimension of the tank, such as the tank diameter. The validity of this nondimensionalization must be checked by an experiment where the container size, configuration, liquid properties, and gravity field are varied. The term in brackets in equation (15) is commonly called the Bond number B. It represents the ratio of gravitational to surface energy. Examination of equation (15) reveals that the gravitational energy term (third term) will not appreciably affect the liquid configuration compared with surface energy terms for small Bond numbers ($B \ll 1$), while the surface energy terms (first two terms) have little affect for large Bond numbers ($B \gg 1$). The former case is commonly referred to as "zero" gravity. The latter case is common to our everyday experience (e.g., a glass of water on a desk). It should be expected that the important effects on the liquid configuration of varying the Bond number can be determined over a Bond number range of $10^2 > B > 10^{-2}$.

According to equations (15) and (16) the two-dimensional simulator should be able to show the shape of the liquid in a different sized two-dimensional container if the following scaling conditions are met:

(1) The contact angles θ are the same for each two-dimensional container.

(2) The Bond numbers are of equal magnitude for each.

(3) The containers and liquid content are geometrically similar (ref. 13); that is, the corresponding two-dimensional tank dimensions are proportional and the liquid content fraction, based on area, is the same.

Numerous authors (e.g., refs. 1 and 3) have noted these same scaling requirements for three-dimensional containers.

Simulation of Three-Dimensional Tanks

In this section an attempt will be made to determine the three-dimensional tanks that can be studied in the two-dimensional simulator. Nondimensionalize equations (6a) and (7) by the following substitution:

$$z = \zeta \mathcal{L}_a \qquad S_{LV} = \sigma_{LV} \mathcal{L}_a^2$$

$$V = \nu \mathcal{L}_a^3 \qquad S_{SV} = \sigma_{SV} \mathcal{L}_a^2$$

The equations describing the actual case become

$$0 = \delta\left\{ \oint\oint_{s_{LV}} ds + \cos(\theta_a) \oint\oint_{s_{SV}} ds + \underbrace{\left[ng_o\left(\frac{\rho_e}{\sigma_{LV}}\right)\mathfrak{L}^2\right]_a}_{B_a} \iiint_u z\, du \right\} \quad (17)$$

and

$$\iiint_u du = u \quad (18)$$

It has been common practice for engineers to solve two-dimensional axisymmetric problems by assuming them to be approximated by a two-dimensional plane problem so that more simple analytical or graphical solution methods could be employed. This assumption is also made here, with the knowledge that the approximation is best away from the axis of rotation. In other words the assumption is made that the liquid configuration in the two-dimensional simulator is approximately the same as the two-dimensional projection (fig. 1) of the three-dimensional liquid configuration in a geometrically similar axisymmetric three-dimensional tank. Based on the previous scaling results, it would be expected that the actual three-dimensional case and the simulator case should be scaled if

(1) The contact angles are equal

$$\theta_a = \theta_s \quad (19)$$

(2) The Bond numbers are equal

$$B_s = B_a$$

or

$$\left[ng_o\left(\frac{\rho_e}{\sigma_{LV}}\right)\mathfrak{L}^2\right]_a = \left[(\sin\varphi)g_o\left(\frac{\rho_e}{\sigma_{LV}}\right)\mathfrak{L}^2\right]_s \left(mg_o \frac{\rho_e}{\sigma_{LV}} \mathfrak{L}^2\right)_s \quad (20)$$

In addition, the two-dimensional projection of the three-dimensional tank should be geometrically similar to the simulator two-dimensional tank and the liquid content fractions, based on two-dimensional projected area or three-dimensional volume (simulator shape rotated 360°), should also be geometrically similar. In order to simulate a three-dimensional tank containing a constant percent full by volume, the amount of liquid in the two-dimensional simulator must be varied some as the effective gravity field m varies.

The validity of the assumptions made in this section must be checked by experiment. Such an experiment would compare drop-tower static liquid configuration data for three-dimensional models (surfaces of revolution) to corresponding simulator data where the effective gravity field, liquid fraction, and

container size and configuration are varied.

Summary of Analysis

The analysis indicated that the two-dimensional shape of the liquid in the plane of the plates of the properly designed two-dimensional simulator should only be affected by the magnitude of gravity, taken as a component, and tank boundaries in that plane. A properly designed simulator requires two parallel flat glass plates that are closely spaced so that the liquid contacts them both and the spacing is far smaller than the local characteristic width of the interface. The analysis indicated that the properly designed simulator should simulate (show) the shape of the liquid in a two-dimensional container. In addition it was assumed that the projected two-dimensional liquid shape in three-dimensional containers (surfaces of revolution) may be approximately simulated by the two-dimensional simulator. Experiments must be performed to validate the assumptions of the analysis.

APPARATUS AND PROCEDURE

Apparatus

Based on the theoretical results previously described, a small simulator was constructed (fig. 3) whose final design and operational procedure, described subsequently, resulted from a series of tests for this purpose. Basically, the device consists of two parallel, flat, glass plates separated by shaped rubber gaskets, which also act as a seal. The gasket is cut to shape to form a scale model of the two-dimensional boundaries of the tank shape of interest.

The glass plate and rubber "sandwich" is clamped to the flat-bed plate (fig. 3) that can be pivoted about an axis. Ideally, when the bed is perfectly level the liquid in the test section (the space between the glass plates and within the gasket boundaries) should assume the zero-gravity shape. When the bed is at an angle to the horizontal φ accomplished by placing a machined spacer under the bed leg, this liquid should assume the corresponding shape for a fraction of 1 g. The bottom glass plate is clamped to the bed by a vacuum between them. The upper glass plate is clamped by another glass-plate gasket-sandwich arrangement, which tends to decrease clamping errors. Closely machined spacers (accuracy $\pm 2.5 \times 10^{-4}$ cm) control the spacing ξ between the glass plates and keep the plates nearly parallel. Liquid contact with the plates is assured by choosing a plate spacing ξ that is less than the "break-away" spacing, which was determined experimentally to be $\xi_{max} = 0.28$ centimeter for ethyl alcohol (see appendix B). All the data in this report were taken with $\xi = 0.152$-centimeter spacers. The glass plates are flat to 2.54×10^{-5} centimeter. The device is leveled by three fine-thread leveling screws.

Ethyl alcohol (200-proof ethanol) has been used as the test liquid for most of the experiments because it is easy to handle and photograph. The alcohol is placed in the test section by a hypodermic needle that pierces the rubber gasket.

Another hypodermic needle is used as a vent. For this experiment the simulator was housed in a room that could not be considered to be a clean room; it was qualitatively about the level of cleanliness of an average household. The plates were cleaned with alcohol and a rubber squeegee every time there was a change in the model.

Ethyl alcohol has a contact angle of $\theta = 0^{\circ}$ on glass and rubber. Nonwetting liquids could, in principle, be used in the simulator. Mercury ($\theta \simeq 125^{\circ}$) was tried; however, dust particles and/or oxidation appeared to affect the flow of this liquid detrimentally to such a degree that this phase of the experiment was dropped. The alcohol exhibited no such difficulties.

Procedure

The two-dimensional tank model centerline is oriented with respect to the gravity vector (downhill direction) to be consistent with the actual case to be simulated (fig. 2). The simulator is leveled (the leveling procedure is discussed in the next section) and an amount of liquid, which will give the geometrically similar liquid content as found in the actual case to be simulated, is injected into the test section. The bed is then stopped from the "leveled" position to a desired bed angle φ, which is between 10^{-4} to $\pi/2$ radians. Stopped positions are obtained by placing spacers between the base plate and the bed leg. The equilibrium (static) liquid shape for various bed angles was observed and photographed.

Leveling Procedure

It is desirable for the test section to be level to a high degree of accuracy ($\varphi = 10^{-4}$ to 10^{-5} rad), and the plates parallel to a comparable accuracy, for low-gravity-field simulation; therefore, a special leveling procedure was developed. Leveling is accomplished by adjusting the leveling screws (fig. 3) until an air bubble injected into an unobstructed liquid area of the test section, moves unmolested by dust, etc. in the opposite direction from the desired gravity vector and at a very slow speed. From the bubble speed U the bed angle can be determined from figure 4 which was derived in appendix C. For example, a bed angle of $\varphi = 10^{-4}$ radian will result in a bubble velocity of $U \simeq 0.3$ centimeter per minute in ethyl alcohol for a spacing of $\xi = 0.152$ centimeter and a bubble radius of $a = 0.64$ centimeter. To aid in this leveling procedure, the bottom glass plate can be initially leveled with a high accuracy level ($\varphi = 0.835 \times 10^{-5}$ rad). It has been experimentally determined that bubble leveling is required, in addition to leveling by a level, at a small bed angle because this method automatically compensates for nonparallel plates caused by irregularities and also because the effective bed angle can be adequately estimated by observing the bubble speed and direction. In other words, the test section itself is used as a level. Machining inaccuracies of the clamps and spacers and the presence of dust particles limited the minimum measurable bed angle to about 5×10^{-5} radian for ethyl alcohol. Once the bed is leveled by this method the experimenter, can then set other bed angles (i.e., stopped positions) from about 10^{-4} to $\pi/2$ radians with good accuracy by merely

inserting appropriate machined spacers between the base plate and the bed leg. After a reduced gravity position or angle is set, the bed can be pivoted to another angle (or gravity field) and returned to the reduced gravity position repeatedly.

Operational Capabilities

The operational capabilities of the two-dimensional simulator discussed herein are summarized as follows:

Time duration possible for experiments	Limitless
Measurable bed angle range, rad	$\pi/2 > \varphi \gtrsim 5\times10^{-5}$
Range of model size (diam), cm	$25 > D_s \gtrsim 2.5$
Contact angle (with air), deg	0 (ethyl alcohol)
Bond number range	$10^4 \gtrsim B_s \gtrsim 2\times10^{-2}$

RESULTS AND DISCUSSION

Scaling

The theoretical analysis indicated that the equilibrium liquid shape in a properly designed two-dimensional simulator should agree with the liquid shape in another geometrically similar two-dimensional container of different size if the contact angles and Bond numbers for each case were equal and the liquid content was geometrically similar. Experiments were performed to determine the validity of this theoretical result.

To check the Bond number scaling over a range of gravity fields, the simulator itself was used. Two different sized, geometrically similar, circular tanks, half full of liquid, were subjected to varying bed angles (effective gravity fields) in the simulator. Figures 5(a) to (c) compare the shape of the liquid in a 7.6-centimeter-diameter circle to the shape occurring in a 12.7-centimeter-diameter circle at the same bed angle (effective gravity field) and also at a bed angle required for correct Bond number scaling. The dark circle seen in the photographs is a reflection of the out-of-focus camera lens, and the two horizontal lines are channels in the bed plate for vacuum distribution. The liquid region of the photographs has been darkened to help the reader distinquish the liquid from the gas. The darkest curved line is the interface while the neighboring lighter curved line is a reflection of the darker line. The effective gravity field is directed toward the bottom of the page. Figures 5(d) to (f) show the result of a similar comparison when the circular tank contains a channel. Figure 5 demonstrates that the shape of the liquid in the 7.6- and 12.7-centimeter-diameter circles is the same only when the Bond numbers are equal. This result is shown most clearly in the center columns of this figure, while the remaining photographs must be superimposed to see this clearly. The practical difficulty with this method of comparison is a result of the fact that changes in the Bond number will greatly affect the liquid shape only at the intermediate Bond numbers, such as those of the center column, where the surface forces and gravity forces are of the same order of magnitude.

Based on figure 5, it can be stated that the Bond number scaling is apparently a valid method to scale the simulator results to a different sized geometrically similar two-dimensional tanks subjected to varying gravity fields. Because only one liquid (ethyl alcohol) has been used in the simulator, contact angle and surface tension were not varied so that a complete check of the scaling parameters for the simulator, indicated in the analysis, could not be performed. Bond number contact-angle scaling is generally accepted (refs. 1 and 3) for three-dimensional containers so that this incompleteness is probably not important.

Simulation of Three-Dimensional Tanks

In this section photographs of several of the two-dimensional static liquid configurations that occurred in the simulator are compared with the two-dimensional photographs of the liquid configuration that occurred in corresponding geometrically similar three-dimensional surface of revolution tanks in the drop tower (ref. 11). Available drop-tower data are presently limited to very small Bond numbers ($B_a < 10^{-3}$, where the gravity field is about 10^{-6} g and the containers are small). Liquid configuration data at the other extreme of very large Bond numbers ($B_a > 10^4$, e.g., where the gravity field is 1 g) requires only desk top observations. As a consequence, data from the two-dimensional simulator and three-dimensional drop-tower liquid configuration (two-dimensional photographs) can only be compared at these two extremes and only for those tank shapes that have been investigated in drop tower studies.

Figures 6 to 8 compare the liquid configuration in three different tank configurations at various liquid content fractions (based on volume) and at zero gravity (very low Bond number).

The two-dimensional containers in the simulator are filled to a level so that the rotation of the two-dimensional area about the centerline will result in the same fractional content (percent full by volume) as for the three-dimensional drop-tower case at a given Bond number. This would normally be done iteratively by first considering the percent full by area equal to the percent full by volume and then tracing the resulting two-dimensional liquid shape that occurs at that Bond number. From this sketch, the rotated percent full by volume could be calculated. By continually correcting the amount of liquid in the simulator until the desired percent full by volume is attained, by rotation of the two-dimensional area, it is possible to obtain a geometrically similar content of liquid (by volume) in the simulator.

Figure 6 indicates good agreement between the simulator and the drop tower considering the fact that the air bubble can be anywhere at zero gravity and the Bond number for the simulator data was not quite as low as for the drop-tower tests. There is good agreement between simulator and drop-tower data for the cylinder and cone (figs. 7 and 8) except for some liquid that formed at the top of the cylinder and cone for the simulator equilibrium data. This discrepancy in equilibrium shapes is probably a result of some "edge effect" for the simulator. In the analysis it was essentially assumed that the plate spacing was much smaller than the local interface width. This assumption would fail where

a narrow width of liquid occurs in the simulator such as the thin layer that slowly flows up the walls of the cylinder and cone in the simulator and forms liquid at the top of these models. The flow up the walls is very slow so that the time to reach the simulator equilibrium shape is considerably longer than the time required to reach the pseudo-equilibrium shape (before flow up the walls) of figures 7 and 8. The size of the pseudo-equilibrium shape then grows smaller as a result of this flow until the simulator equilibrium shape is attained. In most cases this edge effect should prove to be no problem because the flow is very slow in the narrow layers so that the pseudo-equilibrium shape should be recognized readily. No formal comparison is required at very high Bond numbers ($B_a > 10^4$) since the liquid configuration in three-dimensional containers is well known to the reader (the interface is essentially flat, perpendicular to the gravity vector). This flat shape also occurs at correspondingly high Bond numbers in the simulator.

Equilibrium Liquid Configuration Data

Photographs of the equilibrium (static) shape of totally wetting liquid (ethyl alcohol, $\theta = 0^o$) in the simulator, for various two-dimensional tank configurations and bed angles, were taken. These photographs (figs. 9 to 15), when scaled, can be taken to portray (show) approximately the two-dimensional projected liquid shape (fig. 1) in corresponding three-dimensional tanks (surfaces of revolution) when the edge effect contribution is ignored. Each figure is for a constant projected liquid area fraction rather than for a constant liquid volume fraction.

Figures 9 to 11 show the approximate two-dimensional simulator equilibrium shape of the liquid (shaded areas) at various Bond numbers (based on diameter) in a 12.7-centimeter-diameter circle (sphere) and a rectangle (cylinder, L/D = 1.55 and 9.5 cm in diam). The lowest Bond number results were necessarily obtained with a 2.54-centimeter model because the bed angle could not be made small enough to reach the desired Bond number without reducing the model size. These two-dimensional results can be scaled by the Bond number scaling parameter to larger geometrically similar two-dimensional (three dimensional) tanks at various gravity fields. For example, figures 9 and 10 show the liquid shape approximately in a 2.5-meter-diameter circle (sphere), partly filled with ethyl alcohol, at gravity fields of 2×10^{-4}, 2.7×10^{-6}, 2.3×10^{-6}, 2.7×10^{-7}, and 1×10^{-8} in the order of decreasing Bond number. Figure 12 depicts the effect on the liquid configuration of the diameter N of an open-end channel (cylinder) inside a rectangular (cylindrical) tank. The liquid tends to fill the narrower region. Figures 11 and 12, which are simulator equilibrium data, show further examples of the result of the edge effect problem previously discussed. Actually the edge effect problem occurs in all the figures (i.e., the boundaries are wetted) but it does not show up in the photographs except at corners where liquid can build up. Figure 13 demonstrates the equilibrium shape of the liquid in a circle (sphere), with an open-end channel (cylinder), subject to varying gravity fields. Note that the liquid shape tends to become independent of the gravity field direction as the Bond number becomes very small. The results of figures 9 to 12 are in agreement with those of reference 1 for similar situations.

The ability of the two-dimensional simulator to simulate the liquid shape in three-dimensional tanks is demonstrated in figure 13. The results of the smallest bed angle are compared with the drop tower results in figure 14. Figure 15 depicts the shape of liquid at various Bond numbers in a typical rocket propellant tank that is 14 percent full (based on projected area).

CONCLUDING REMARKS

The two-dimensional simulator discussed in this report appears to be able to show the approximate equilibrium liquid shape in many surface-of-revolution containers over a range of tank size and gravity field when scaled by the Bond number and the proper procedure is used in its operation and interpretation of its data. This device has some advantages over other methods when the approximate liquid shape over the significant Bond number range is desired.

Lewis Research Center,
National Aeronautics and Space Administration,
Cleveland, Ohio, October 7, 1965.

APPENDIX A

SYMBOLS

A	liquid contact area with either upper or lower plates, sq cm
A_T	area of plate within model boundaries, sq cm
a	bubble radius, cm
$\mathcal{a}$	nondimensional area, $\equiv A/\mathfrak{L}_s^2$
B	Bond number
C	length of curve, cm
C_D	effective drag coefficient for bubble
$\mathcal{c}$	nondimensional length variable, $\equiv s/\mathfrak{L}$
D	characteristic tank diameter, cm
e	constant
F_B	bouyant force, dynes
F_D	drag force, dynes
g_o	constant acceleration due to gravity, 981 cm/sec^2
I	energy, dyne-cm
K	constant
$\mathfrak{L}$	characteristic length, cm
M,N	baffle spacing defined in fig. 12
m	n sin φ, number of gravities component in opposite direction of α (fig. 2); n = 1 for simulator, therefore, m = sin φ
n	number of gravities in opposite direction of z (fig. 2)
R_M^*	modified Reynolds number, $\equiv (U\xi/\nu_l)(\xi/a)^{1/2}$
r	radial coordinate
S	surface area, sq cm
s	distance along surface, cm

$\mathcal{A}$	nondimensional surface area, $\equiv S/\mathcal{L}^2$
t	time, sec
U	bubble velocity, cm/sec
V	volume of the liquid, cu cm
$\mathcal{V}$	nondimensional liquid volume, $\equiv V/\mathcal{L}_a^3$
x	direction parallel to pivot axis, cm
z	height above reference horizontal plane, parallel to gravity vector, cm
$\mathcal{Z}$	nondimensional liquid depth; this term includes cosine of angle between axis of rotation and gravity field, $z/\mathcal{L}_a$ or $\alpha/\mathcal{L}_s$
α	liquid depth in simulator with direction parallel to plates and perpendicular to pivot axis (fig. 2), cm
β	direction perpendicular to plane of plates (fig. 2), cm
θ	contact angle, deg or rad
ν	kinematic viscosity, sq cm/sec
ξ	spacing between plates, cm
ρ	mass density, g/cu cm
ρ_e	buoyant mass density, $\rho_l - \rho_f$, g/cu cm
Σ_j	sum over j
σ	surface tension or surface free energy per unit area, dyne/cm
φ	angle simulator bed makes from horizontal, rad or deg
$\int, \oint_C, \oint\oint_A, \iiint_V$	integrals: standard, along curve C, over surface A, over volume V

Subscripts:

a	actual
B	model boundary surface - solid surface not including plates

b	boundary surface - all solid surfaces enclosing fluid
f	other fluid, in this case air
i	pertaining to interface
j	summing subscript to include all surfaces
l	liquid
LS	liquid-solid interface
LV	liquid-vapor interface
max	maximum
min	minimum
p	surface area of plates within model boundaries
SLB	solid-liquid interface on model boundary
SV	solid-vapor interface
SVB	solid-vapor interface on model boundary
SVP	solid-vapor interface on plates
s	simulated case

APPENDIX B

DISCUSSION OF PLATE SPACING

The assumption concerning the constancy of the cross-sectional area ($A(x,\alpha)$, fig. 2) of the liquid in the planes of the plates requires some additional justification. A simple experiment with a drop of wetting liquid (ethyl alcohol) between the two glass plates can be used to show that liquid contacts the top and bottom plates when the plate spacing ξ is below a critical value ξ_{max}. Figure 16 describes the liquid (ethyl alcohol) shape as ξ increases up to $\xi_{max} \simeq 0.28$ centimeter, after which liquid contact with the plates is lost. Clearly the variation of the cross-sectional area $A(x,\alpha)$ with β is small for large $\mathfrak{L}/\xi$, as long as there is contact. This is assured for $\xi < \xi_{max}$. A nonwetting liquid should give qualitatively similar results; however, the interface curvature would be reversed.

The maximum plate spacing ξ_{max} that allows liquid to contact the plates can be estimated for a wetting liquid by equating the potential energy of the liquid before contact is lost to the surface energy of the two free surfaces that occur just after contact is lost. Thus

$$\iiint_V (\cos \varphi)\rho g_o z \, dV \simeq 2 \int_A \sigma_{LV} \, dA \qquad \text{for} \quad \mathfrak{L}/\xi \gg 1 \tag{B1}$$

Since the cross-sectional area A is essentially independent of the liquid depth, the relation simplifies, for constant properties and horizontal plate ($\cos \varphi = 1$), to

$$\rho g_o \int_0^{\xi_{max}} z \, dz \simeq 2\sigma_{LV} \tag{B2}$$

or

$$\xi_{max} \simeq \sqrt{\frac{4\sigma_{LV}}{\rho g_o}} \tag{B3}$$

Experimental values of ξ_{max} are compared in table I with values derived from equation (B3).

TABLE I. - APPROXIMATE VALUES OF ξ_{max} FOR SOME COMMON LIQUIDS

Liquid	Experimental, ξ_{max}, cm	Calculated, ξ_{max}, cm
Ethyl alcohol	0.28	0.30
Ethylene glycol	.33	.44
Water	.43	.54

APPENDIX C

LEVELING

Parallel Plates

The velocity of an air bubble injected into the liquid can be used to determine the angle of parallel plates to the horizontal (fig. 17). The air bubble should be large enough to contact both plates and should be injected into a relatively unrestricted region of the liquid.

Assume that the predominant forces acting on the nearly cylindrical air bubble are the buoyant force and an effective drag force due to form drag of the bubble and drag by the plates on the liquid moved by the bubble. The buoyant force on a bubble of radius a is

$$F_B = \pi a^2(\rho_l - \rho_f)g_o \xi n \sin \varphi \tag{C1}$$

where

$$n = 1$$

The effective drag force on the bubble is

$$F_D = C_D \rho_l 2a \frac{U^2}{2} \xi \tag{C2}$$

where C_D is the drag coefficient, which is taken to be a function of a Reynolds number, of the form

$$C_D = K(R_M^*)^e \tag{C3}$$

Assume a modified Reynolds number of the form

$$R_M^* \equiv \frac{U\xi}{\nu_l}\left(\frac{\xi}{a}\right)^{1/2} \tag{C4}$$

Equating the buoyant and effective drag forces and substituting equations (C3) and (C4) into that result give

$$U^2 = \frac{\pi(\rho_l - \rho_f)g_o a \sin \varphi}{\rho_l K\left[\frac{U\xi}{\nu_l}\left(\frac{\xi}{a}\right)^{1/2}\right]^e} \tag{C5}$$

Experimental data for ethyl alcohol and glycerine at various bed angles and

bubble sizes were correlated by equation (C5) when the following values of K and e were chosen: $K \simeq 180$ and $e \simeq -1$. Using the preceding values for K and e simplifies equation (C5) to

$$U \simeq \left[\frac{\pi(\rho_l - \rho_f)g_o(\xi)^{3/2}}{180\ \rho_l \nu_l}\right] a^{1/2} \sin \varphi \qquad (C6)$$

A plot of experimental data for bed-angle bubble size (i.e., $a^{1/2} \sin \varphi$) as a function of bubble speed for ethyl alcohol and glycerine (corrected by equation (C6) for viscosity) is given in figure 4.

The accuracy of this method in determining the bed angle at low bed angles, as estimated by the scatter of the data in figure 4, is about ±30 percent. At low Bond numbers, which correspond to low bed angles, inaccuracies of this order in the bed angle would not result in noticeable changes in the liquid shape in the two-dimensional model tank. Therefore this method of estimating the low bed angles should be adequate for this purpose.

Plates Canted

Plate canting (i.e., nonparallel plates) caused by machining inaccuracy in the spacers and nonuniform clamping can affect the liquid shape for bed angles below about 5×10^{-3} radian. The canting angle error can be compensated for by adjusting the level. The combined effect of nonlevel parallel plates and canted plates (effective bed angle) can be estimated by the velocity of an air bubble by using equation (C6).

REFERENCES

1. Otto, E. W.: Static and Dynamic Behavior of the Liquid-Vapor Interface During Weightlessness. Paper No. 17a, A.I.Ch.E., 1965.

2. Paynter, Howard L.; Mackenzie, C. Malcolm; Marsh, Ralph A.; and Tyler, Vernal M.: Zero G Liquid Propellant Orientation by Passive Control. Paper No. 862D, SAE, 1964.

3. Li, Ta: Hydrostatics in Various Gravitational Fields. J. of Chem. Phys., vol. 36, no. 9, May 1, 1962, pp. 2369-2375.

4. DiMaggio, O. D.: Equilibrium Configuration of the Liquid-Vapor Interface in a Rotating Container Under Zero G Conditions. Vol. 14 of Advances in Astronaut. Sci., E. T. Benedikt and R. W. Halliburton, eds., Western Periodicals Co., 1963, pp. 38-48.

5. Petrash, Donald A.; Nelson, Thomas M.; and Otto, Edward W.: Effect of Surface Energy on the Liquid-Vapor Interface Configuration During Weightlessness. NASA TN D-1582, 1963.

6. Petrash, Donald A.; and Otto, Edward W.: Studies of the Liquid-Vapor Interface Configuration in Weightlessness. Paper No. 2514-62, ARS, 1962.

7. Hele-Shaw, H. S. S.: Investigation of the Nature of Surface Resistance of Water and of Stream Motion Under Certain Experimental Conditions. Trans. Inst. Naval Architects, vol. 40, 1898, pp. 25-46.

8. Saffman, P. G.; and Taylor, Geoffrey: The Penetration of a Fluid into a Porous Medium or Hele-Shaw Cell Containing a More Viscous Liquid. Proc. Roy. Soc. (London), ser. A, vol. 245, no. 1242, June 28, 1958, pp. 312-329.

9. Landau, L. D.; and Lifshitz, E. M.: Fluid Mechanics. Addison-Wesley Pub. Co., 1959, pp. 230-237.

10. Rouse, H.: Elementary Mechanics of Fluids. John Wiley & Sons, Inc., 1946, ch. X.

11. Petrash, Donald A.; Nussle, Ralph C.; and Otto, Edward W.: Effect of Contact Angle and Tank Geometry on the Configuration of the Liquid-Vapor Interface During Weightlessness. NASA TN D-2075, 1963.

12. McCuskey, S. W.: Introduction to Advanced Dynamics. Addison-Wesley Pub. Co., 1959, p. 46.

13. Bird, R. B.; Stewart, W. E.; and Lightfoot, E. N.: Transport Phenomena. John Wiley & Sons, Inc., 1960, pp. 107-111.

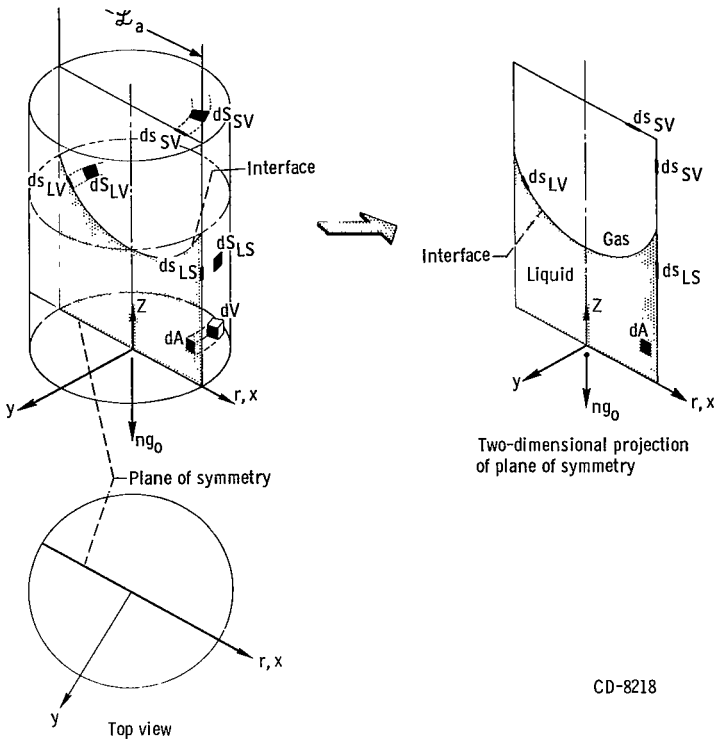

Figure 1. - Schematic drawing of liquid configuration in three-dimensional tank.

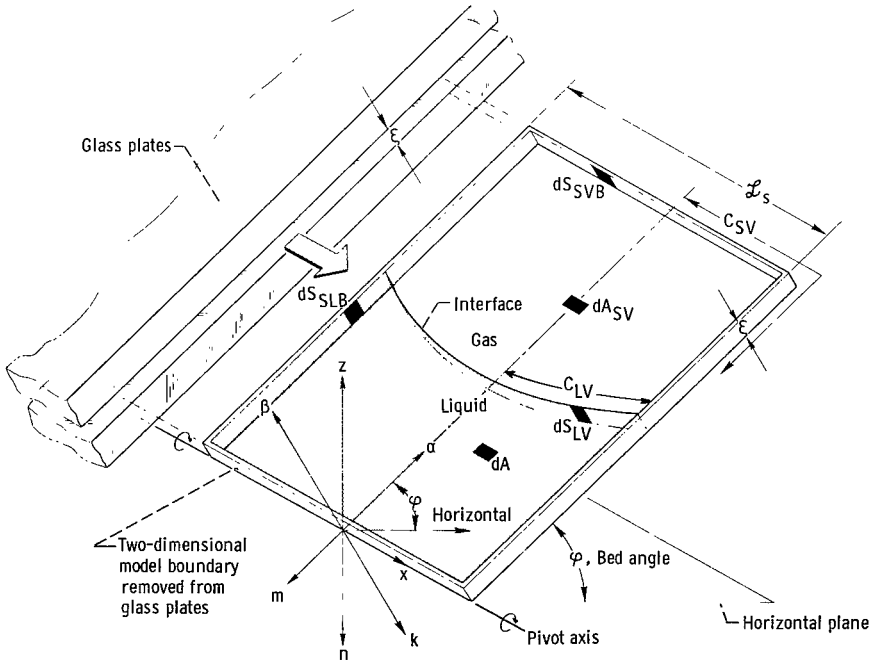

Figure 2. - Schematic drawing of two-dimensional reduced gravity liquid configuration in simulator.

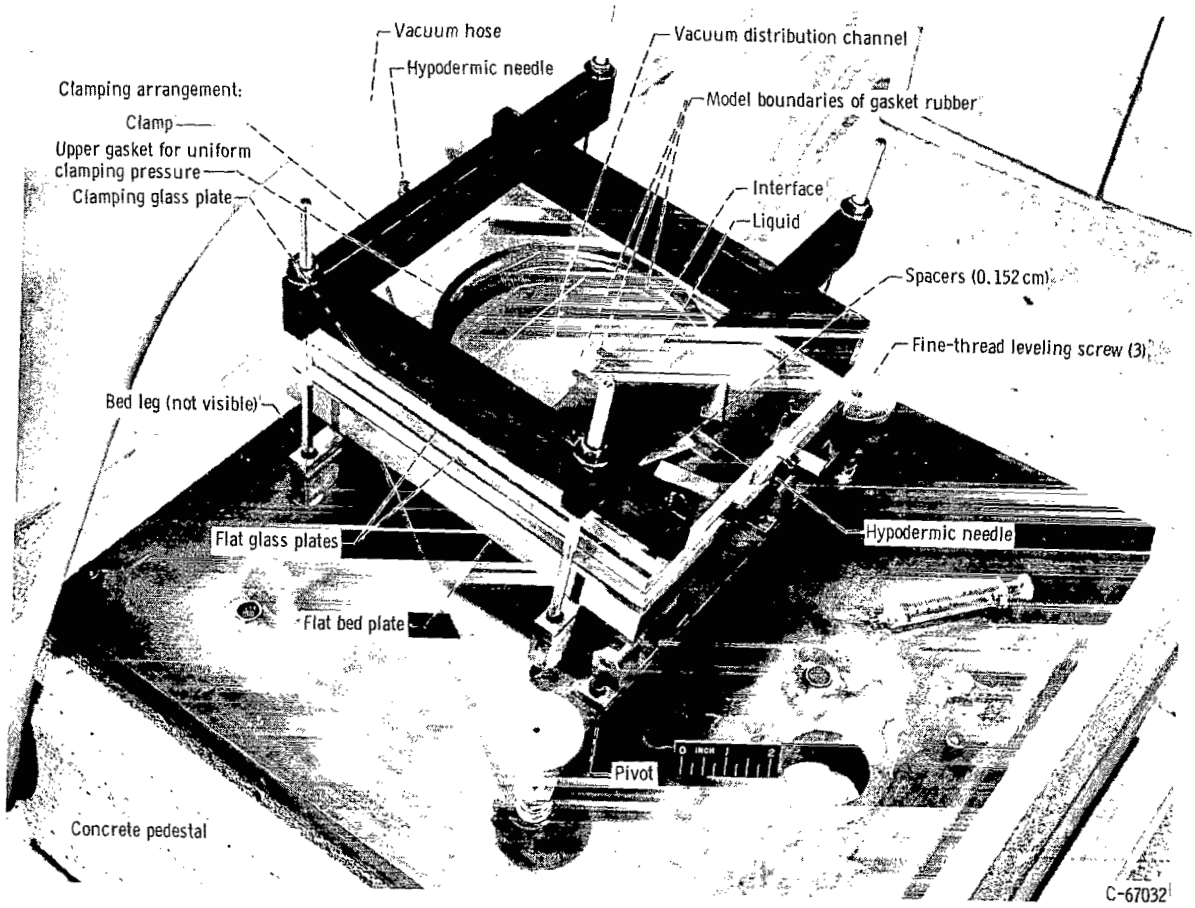

(a) Overall view.

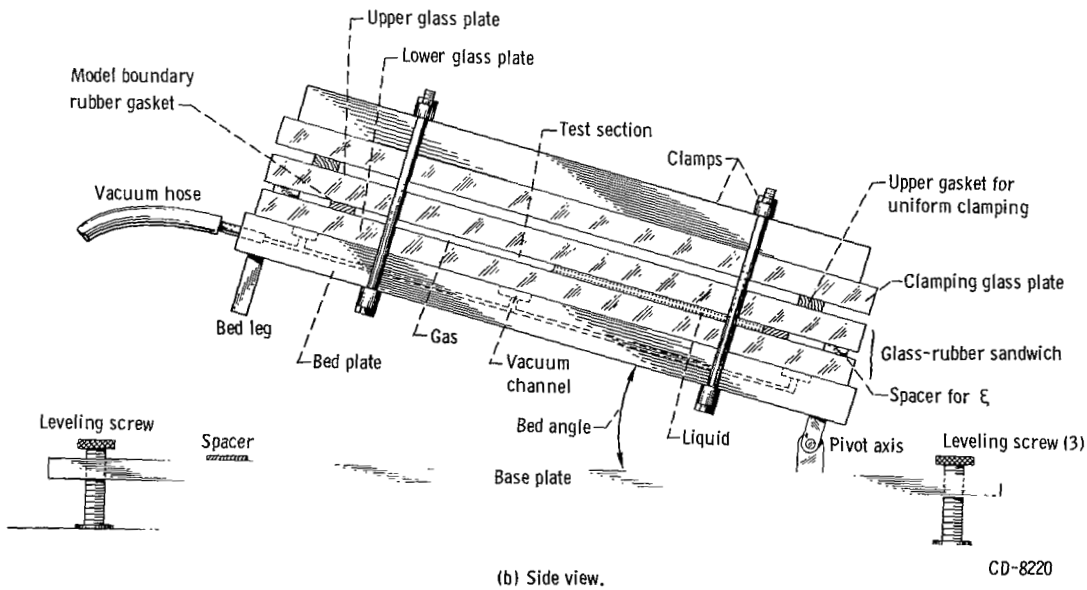

(b) Side view.

Figure 3. - Two-dimensional reduced gravity simulator at bed angle of 10^{-1} radian (angle exaggerated).

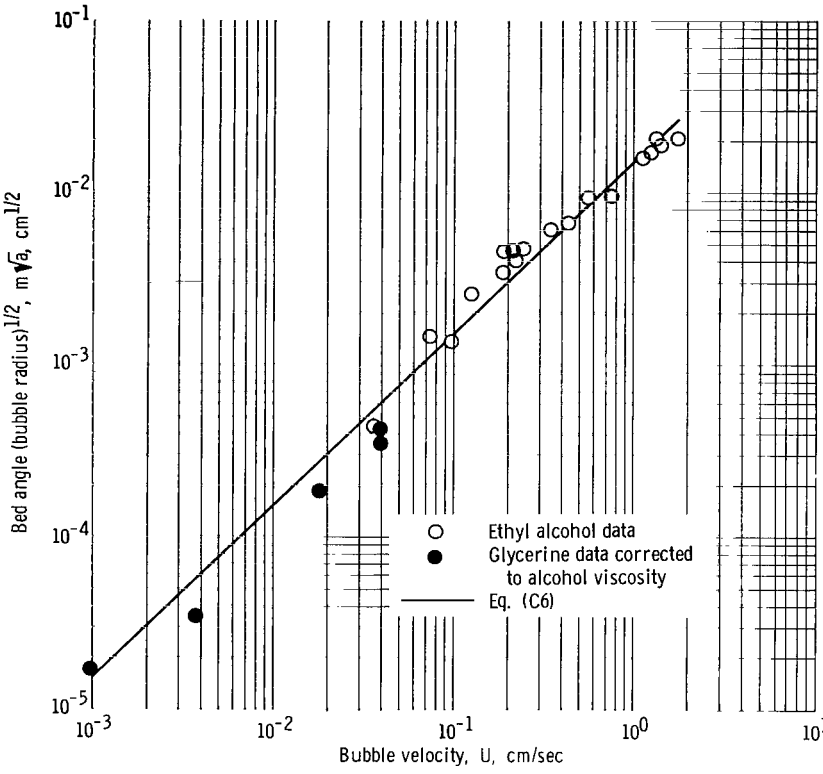

Figure 4. - Curve to determine low bed angles from bubble speed measurements for alcohol with 0.152-centimeter plate spacing.

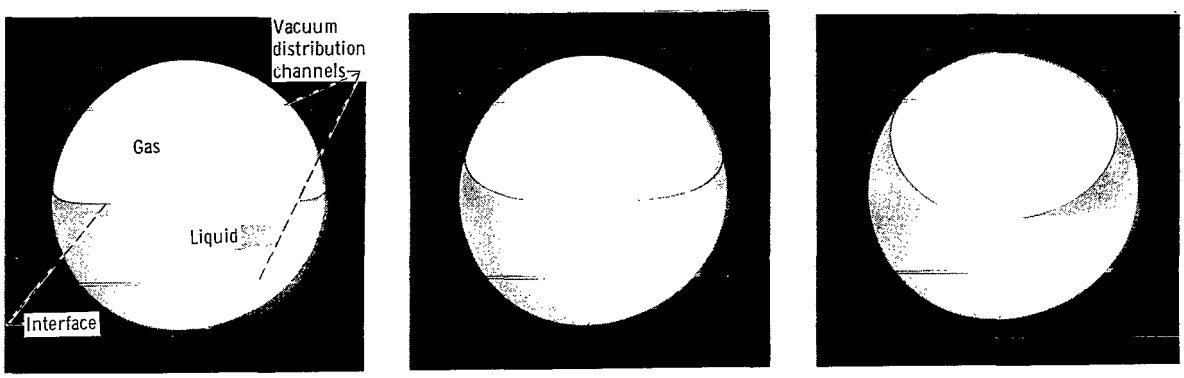

Bond number:	460	60	5.15
Bed angle:	$0.84X10^{-1}$ rad	$1.1X10^{-2}$ rad	$8.9X10^{-4}$ rad

(a) 12.7-Centimeter-diameter circle at various bed angles.

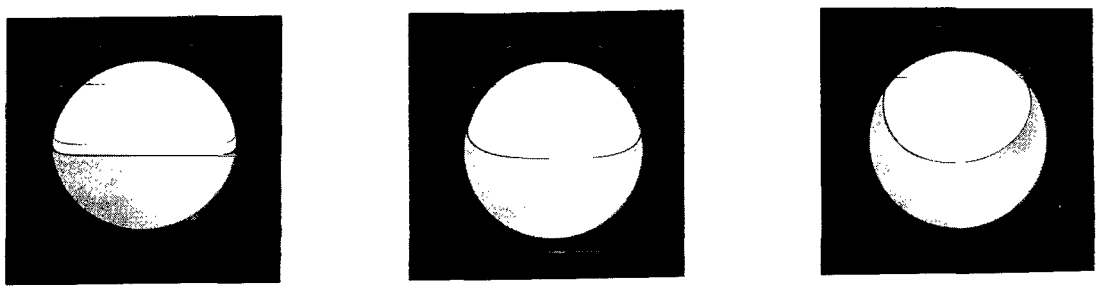

Bond number:	460	60	5.15
Bed angle:	$2.29X10^{-1}$ rad	$2.97X10^{-2}$ rad	$2.56X10^{-3}$ rad

(b) 7.6-Centimeter-diameter circle with bed angle set so that Bond number is same as for 12.7-centimeter circle.

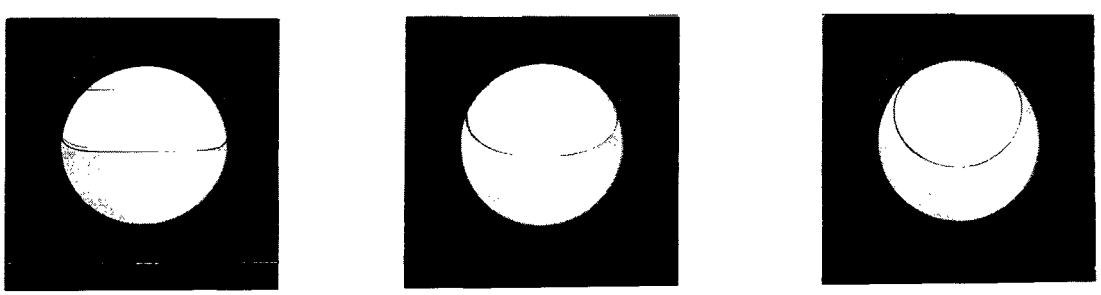

Bond number:	169	22	1.79
Bed angle:	$0.84X10^{-1}$ rad	$1.1X10^{-2}$ rad	$8.9X10^{-4}$ rad

C-65-3608

(c) 7.6-Centimeter-diameter circle with same bed angle as 12.7-centimeter circle.

Figure 5. - Comparison of liquid configuration in two different size half-full (based on area) circles.

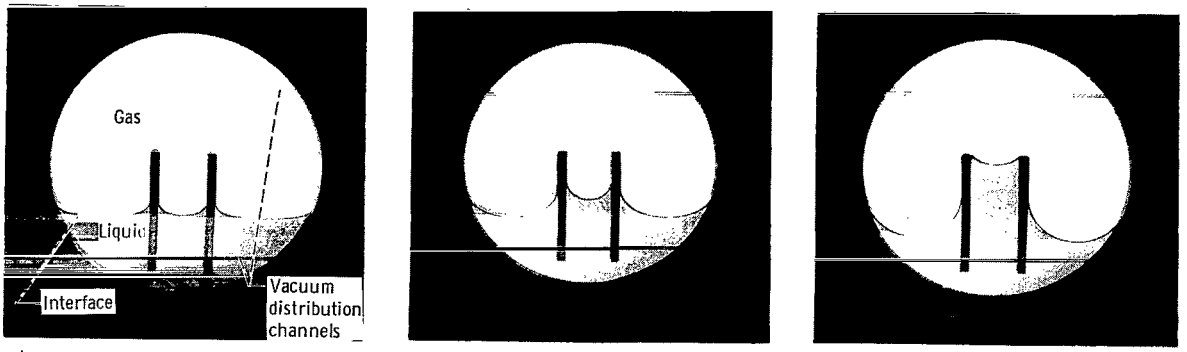

Bond number:	460	60	5.15
Bed angle:	$0.84X10^{-1}$ rad	$1.1X10^{-2}$ rad	$8.9X10^{-4}$ rad

(d) 12.7-Centimeter-diameter circle at various bed angles.

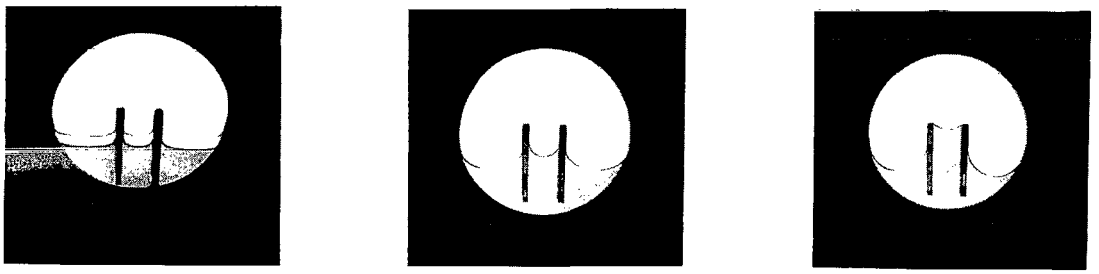

Bond number:	460	60	5.15
Bed angle:	$2.29X10^{-1}$ rad	$2.97X10^{-2}$ rad	$2.56X10^{-3}$ rad

(e) 7.6-Centimeter-diameter circle with bed angle set so that Bond number is same as for 12.7-centimeter circle.

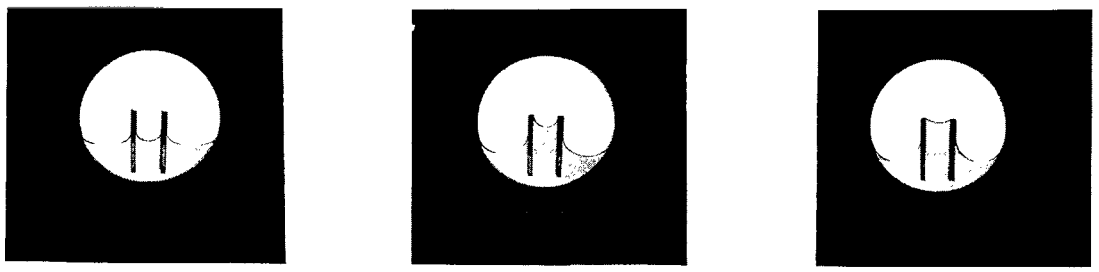

Bond number:	169	22	1.79 C-65-3608
Bed angle:	$0.84X10^{-1}$ rad	$1.1X10^{-2}$ rad	$8.9X10^{-4}$ rad

(f) 7.6-Centimeter-diameter circle with same bed angle as 12.7-centimeter circle.

Figure 5. - Concluded.

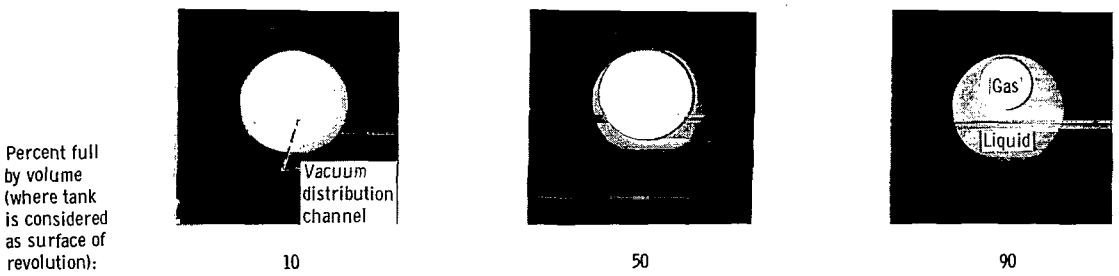

(a) Simulator results. Bond number (based on diam), approximately 0.02.

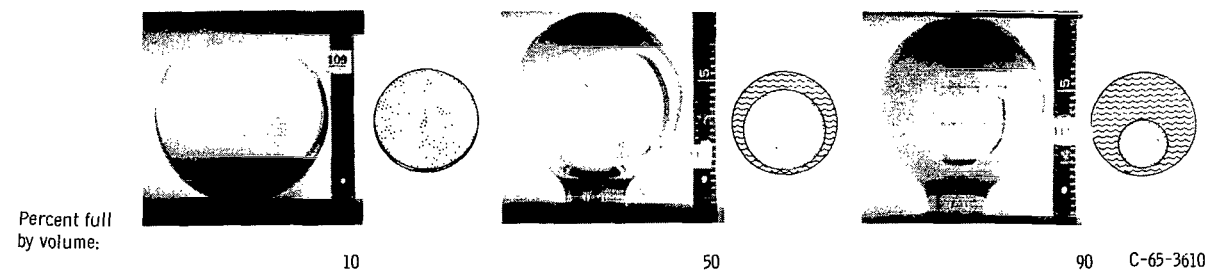

(b) Drop-tower results. Bond number (based on diam), approximately 0.001.

Figure 6. - Comparison of liquid shape in *partially filled sphere* as obtained in drop-tower experiments (ref. 11) to shape observed in two-dimensional projection of container in simulator at essentially zero gravity. Sketch is interpretation of adjoining photograph by authors of reference 11.

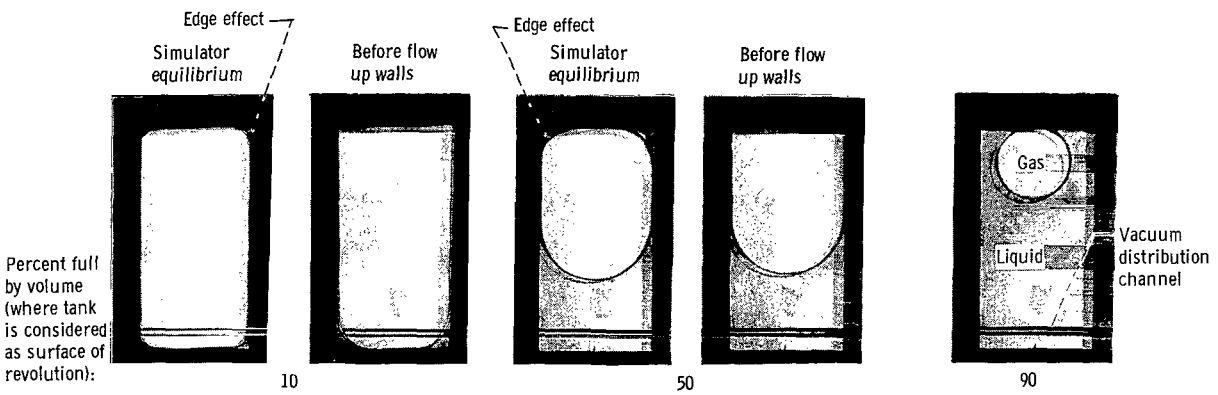

(a) Simulator results. Bond number (based on tank diam), approximately 0.02.

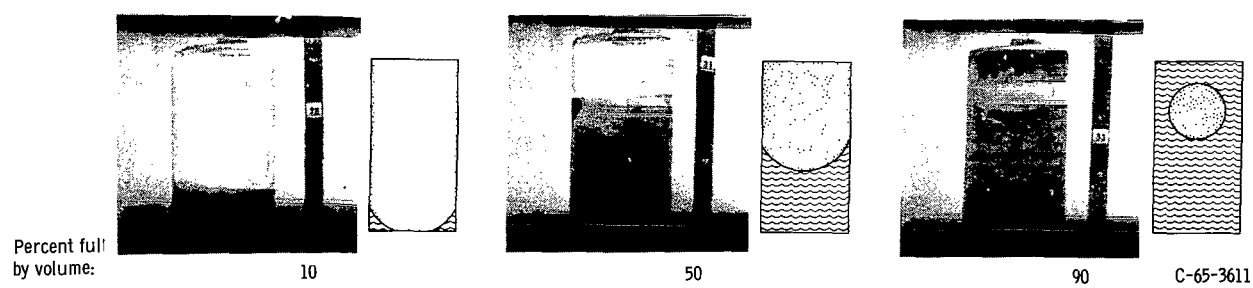

(b) Drop-tower results. Bond number (based on diam), approximately 0.006.

Figure 7. - Comparison of liquid shape in partially filled cylinder as observed in drop-tower experiments (ref. 11) to shape observed in two-dimensional projection of container in simulator at essentially zero gravity.

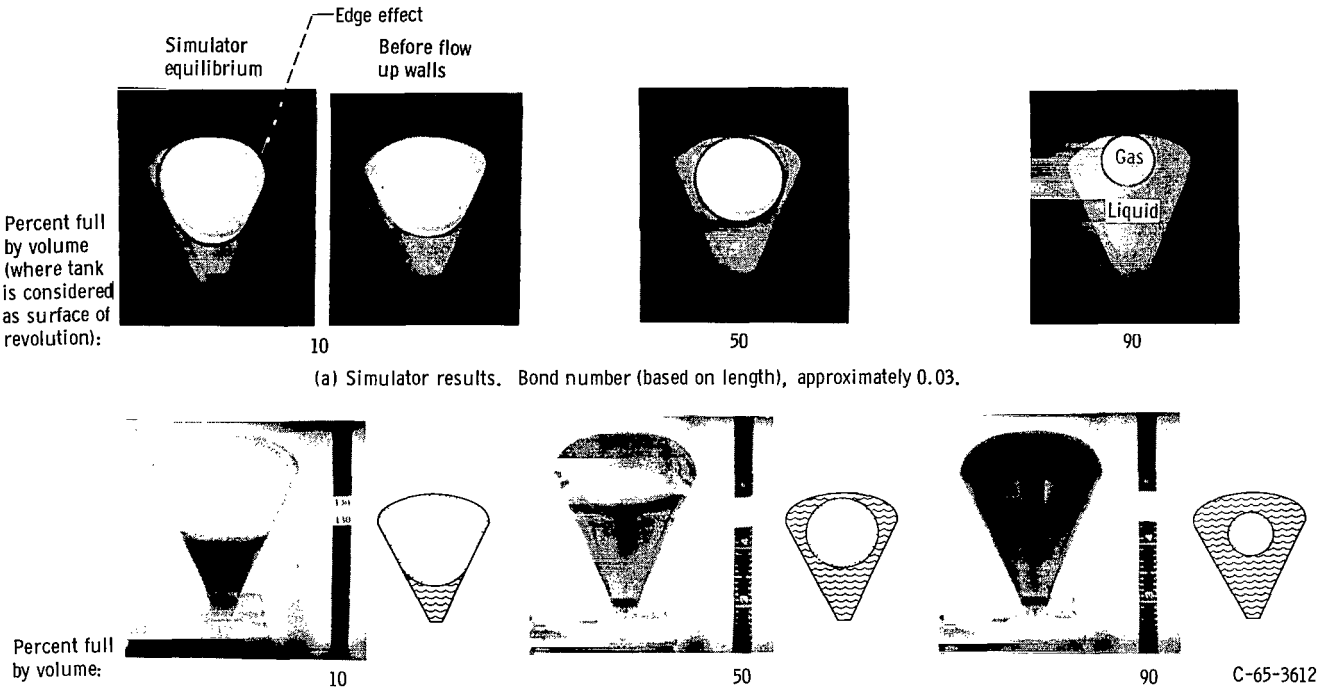

(a) Simulator results. Bond number (based on length), approximately 0.03.

(b) Drop-tower results. Bond number (based on maximum diam), approximately 0.0015.

Figure 8. - Comparison of liquid shape in partially filled cone as obtained in drop-tower experiments (ref. 11) to shape observed in two-dimensional projection of container in simulator at near zero gravity.

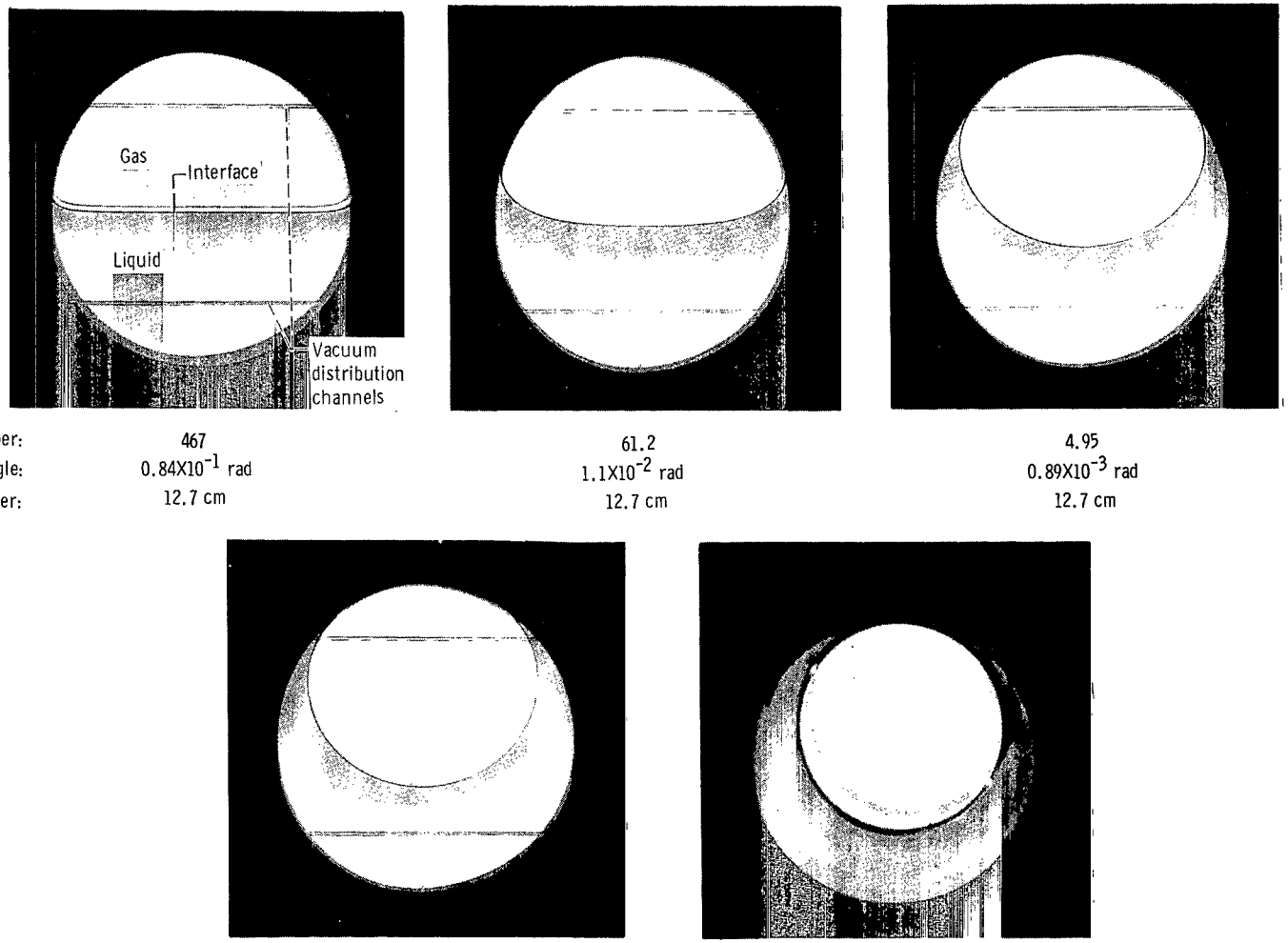

Figure 9. - Two-dimensional simulator equilibrium liquid configuration in half-full (based on projected area) circular (spherical) tanks at various Bond numbers.

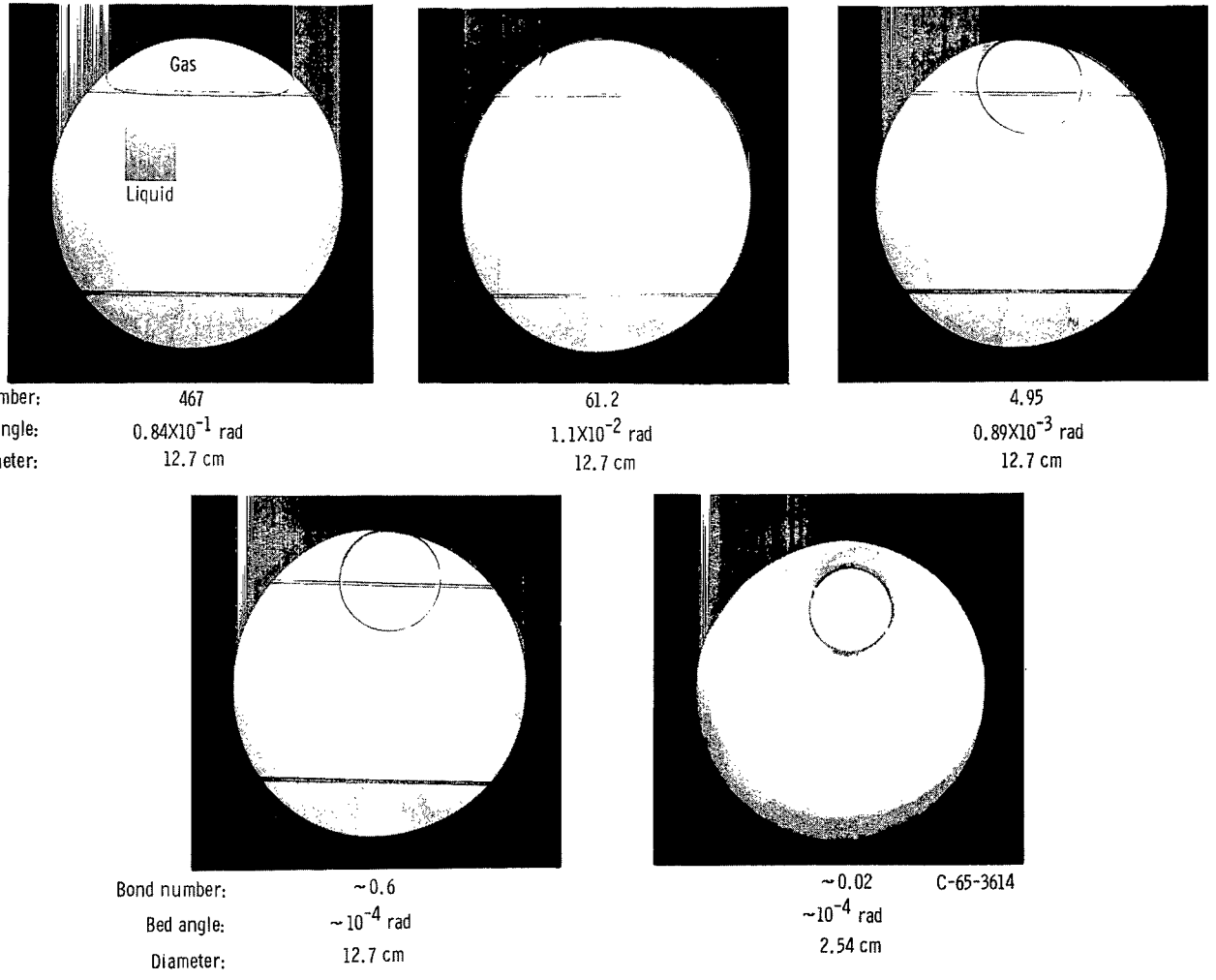

Figure 10. - Two-dimensional simulator equilibrium liquid configuration in 90-percent-full (based on projected area) circular (spherical) container at various Bond numbers.

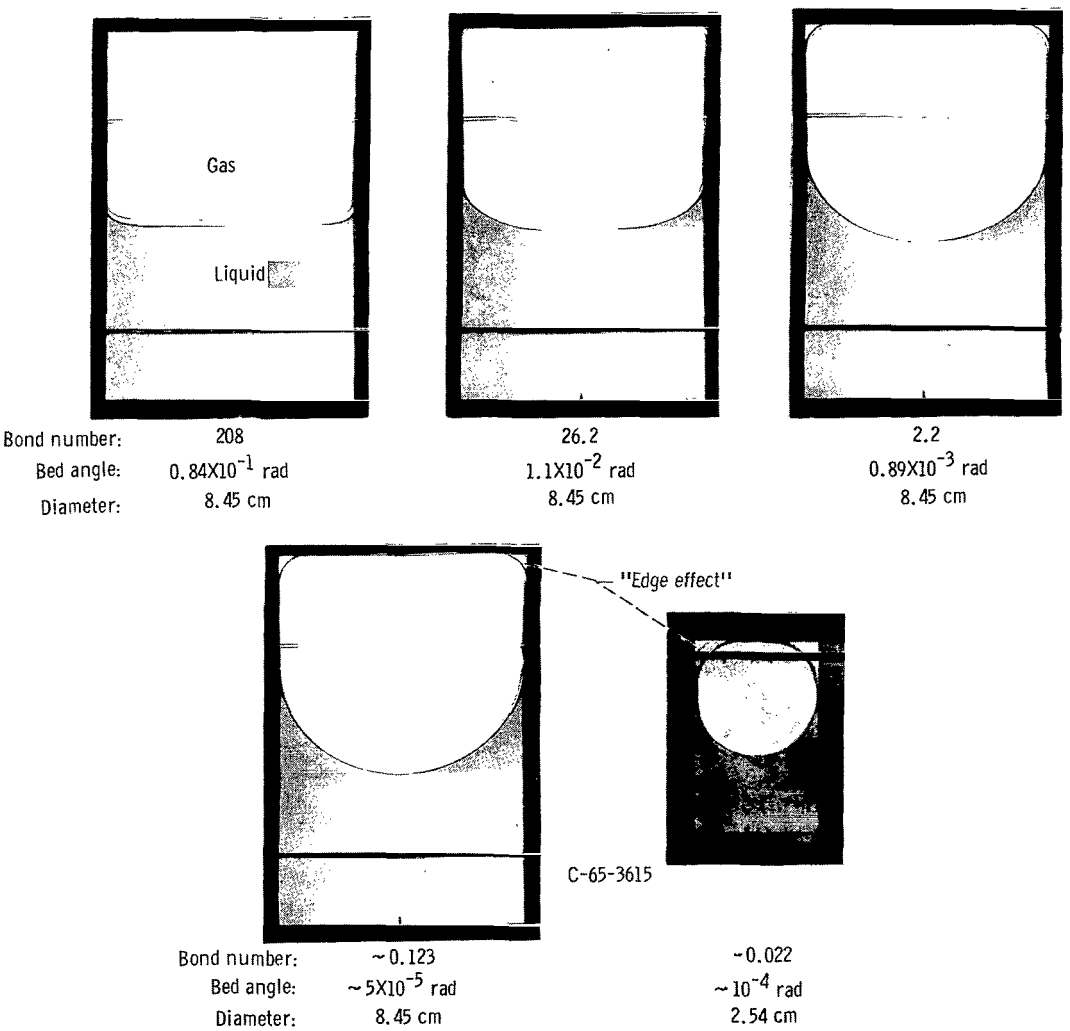

Figure 11. Two-dimensional simulator equilibrium liquid configuration in half-full (based on projected area) rectangular (cylindrical) container (L/D = 1.55) at various Bond numbers.

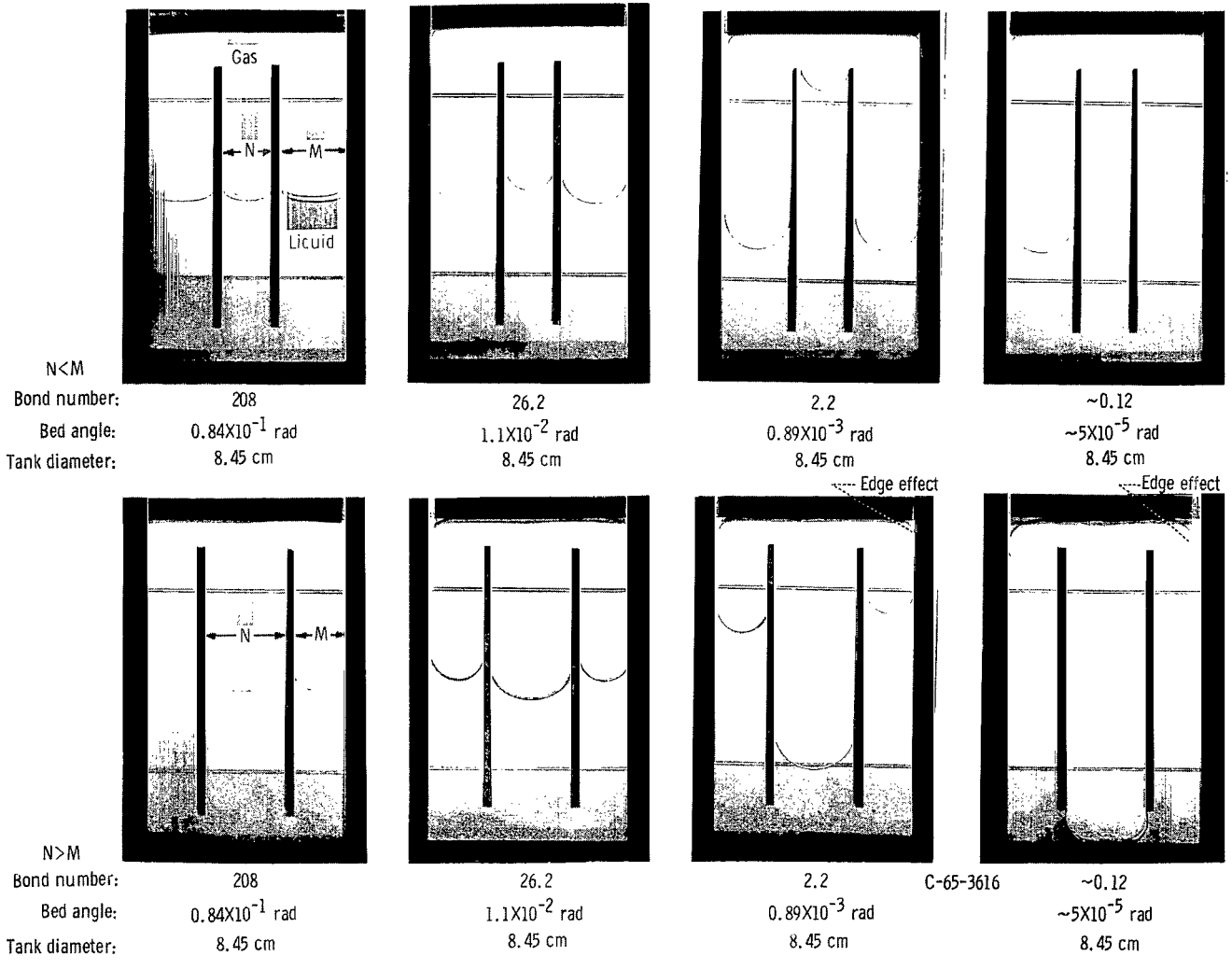

Figure 12. - Effect of an internal baffle (cylinder) on simulator equilibrium liquid shape in half-full (based on projected area) rectangular (L/D = 1.55) container at various Bond numbers.

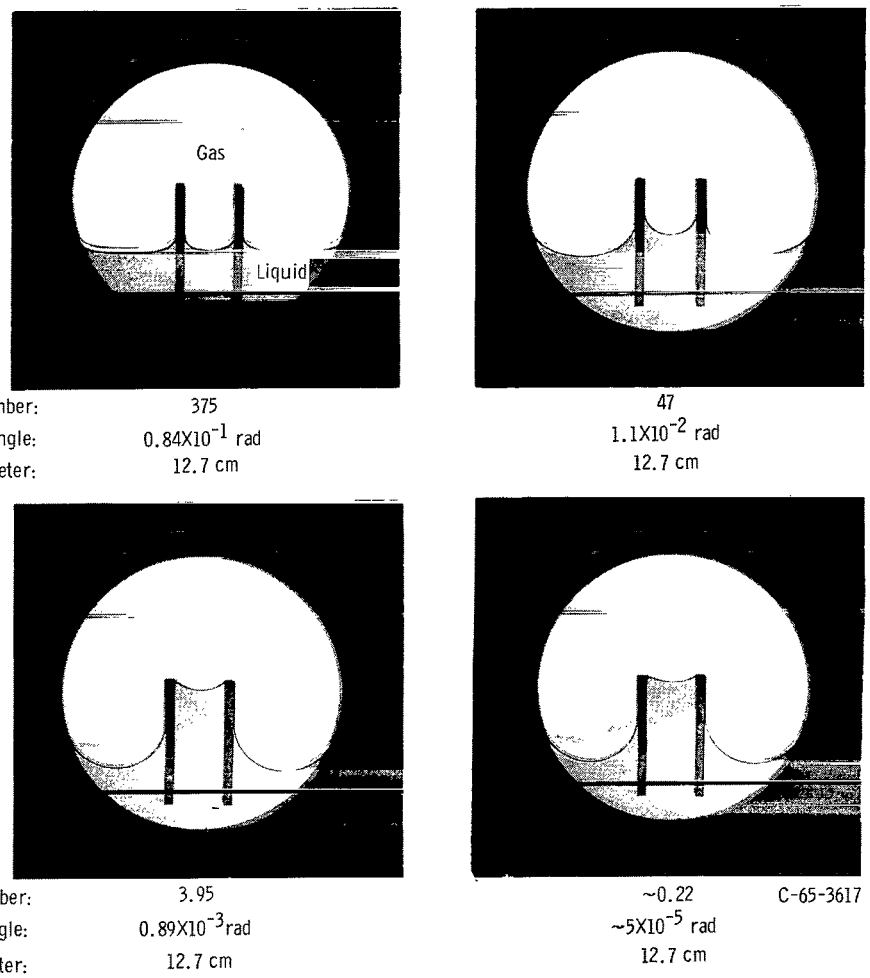

(a) Channel (open-end cylinder) axis parallel to direction of gravity field.

Figure 13. - Two-dimensional simulator equilibrium liquid configuration in 25-percent-full (based on projected area) circular (spherical) tank at various Bond numbers.

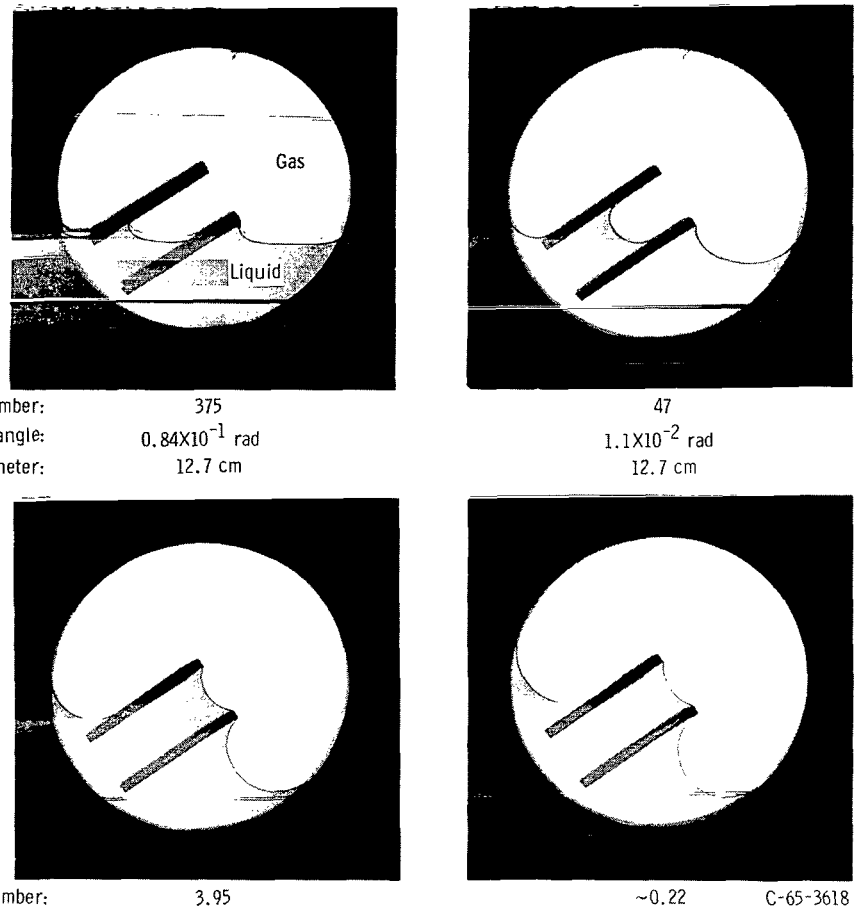

(b) Channel (open-end cylinder) axis 45° from direction of gravity field.

Figure 13. - Continued.

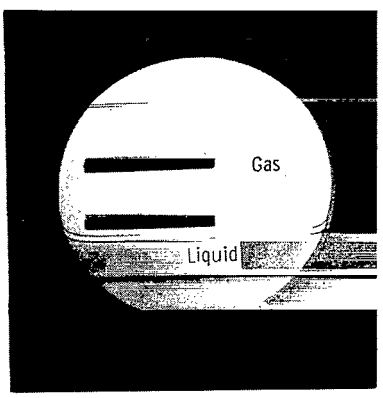

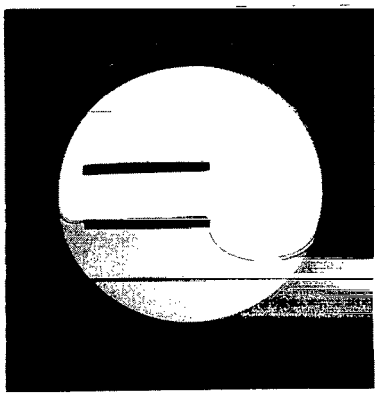

Bond number: 375 47
Bed angle: $0.84X10^{-1}$ rad $1.1X10^{-2}$ rad
Tank diameter: 12.7 cm 12.7 cm

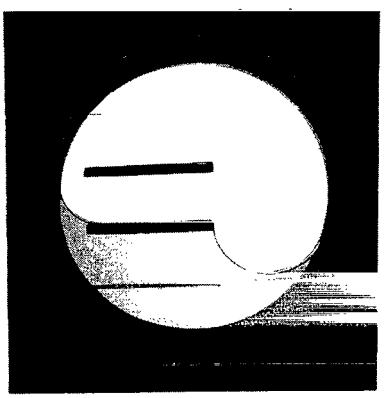

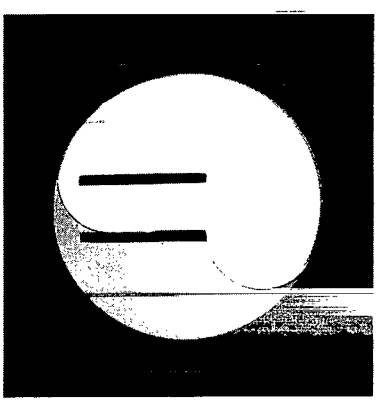

Bond number: 3.95 ~0.22 C-65-3619
Bed angle: $0.89X10^{-3}$ rad $\sim 5X10^{-5}$ rad
Tank diameter: 12.7 cm 12.7 cm

(c) Channel (open-end cylinder) axis is 90° from direction of gravity field.

Figure 13. - Concluded.

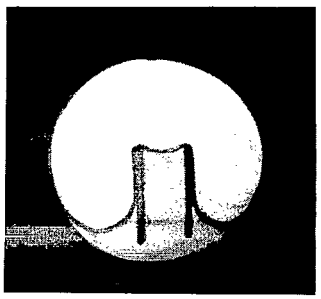

Bond number: ~0.022
Bed angle: ~10^{-4} rad
Tank diameter: 2.54 cm

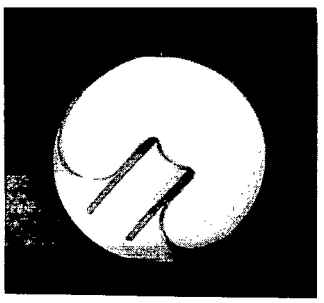

~0.022
~10^{-4} rad
2.54 cm

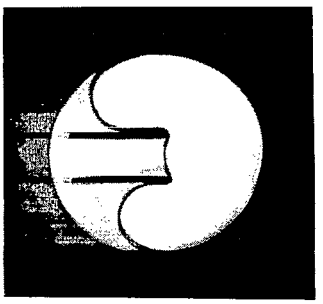

~0.022
~10^{-4} rad
2.54 cm

(a) Simulator result.

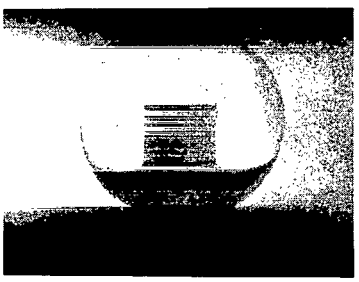

Bond number: ~0.001
Tank diameter: 5.76 cm

~0.001
5.76 cm

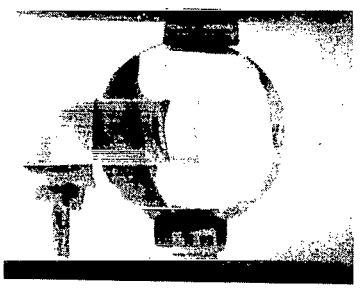

~0.001
5.76 cm
Approaching steady-state zero-gravity configuration

C-65-3620

(b) Drop-tower result (ref. 1).

Figure 14. - Further comparison of results of simulator and drop tower.

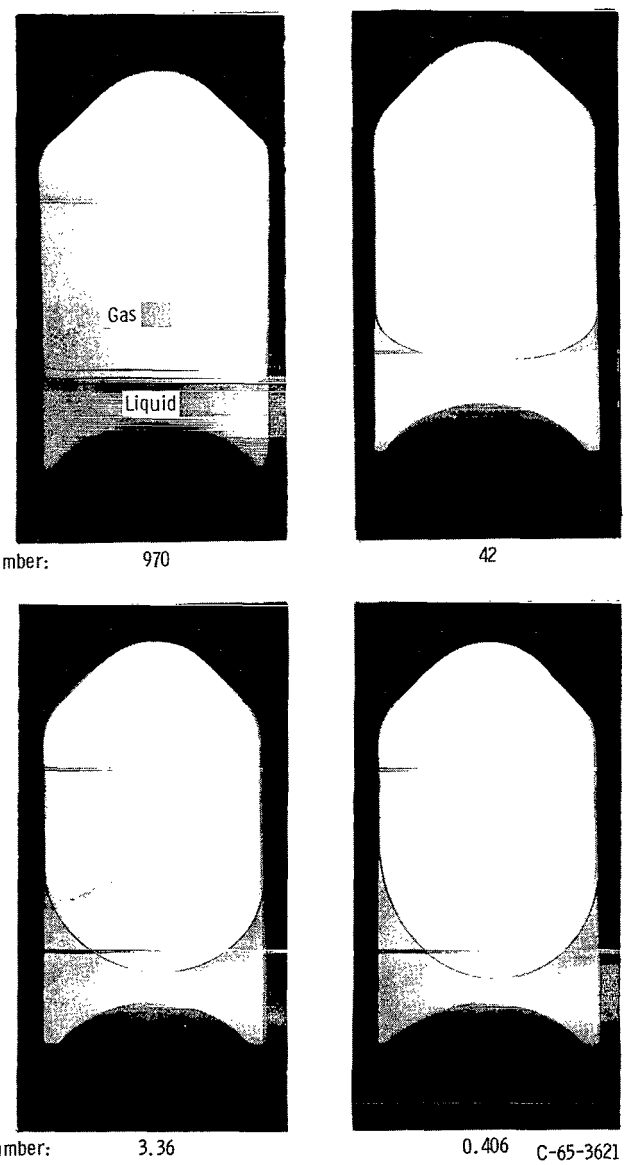

Figure 15. - Two-dimensional simulator equilibrium shape of liquid in two-dimensional model of 14-percent-full (based on projected area) tank at various Bond numbers.

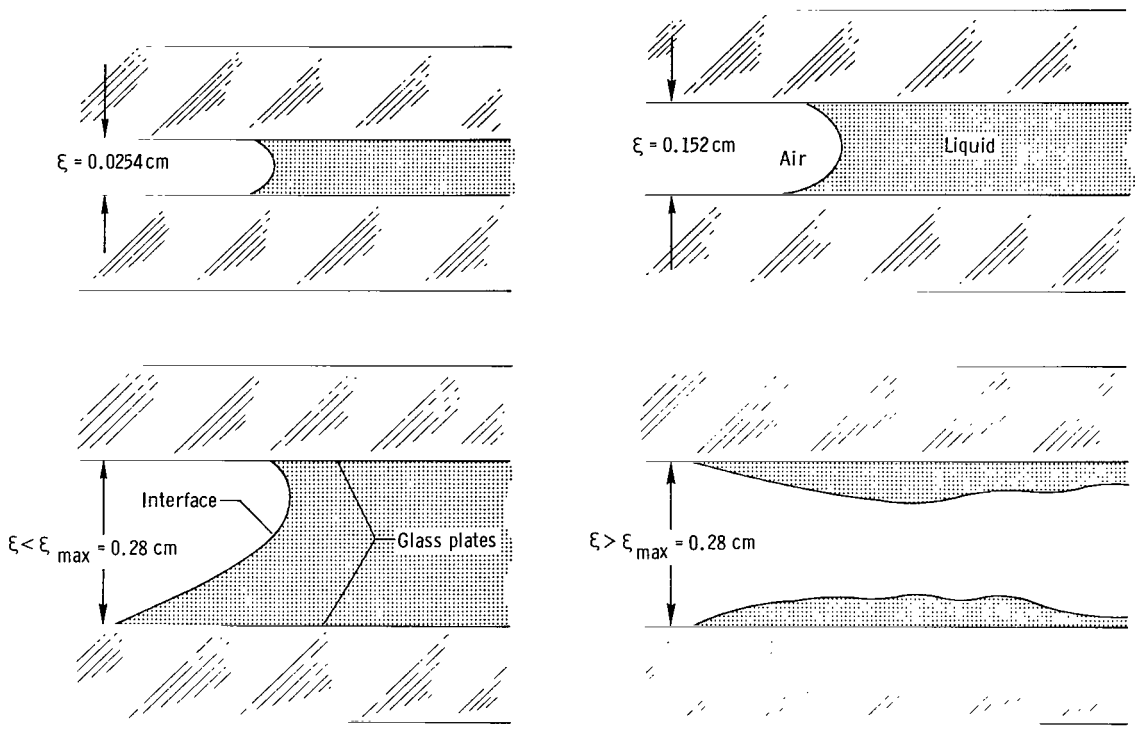

Figure 16. - Effect of plate spacing ξ on liquid shape between plates for ethyl alcohol.

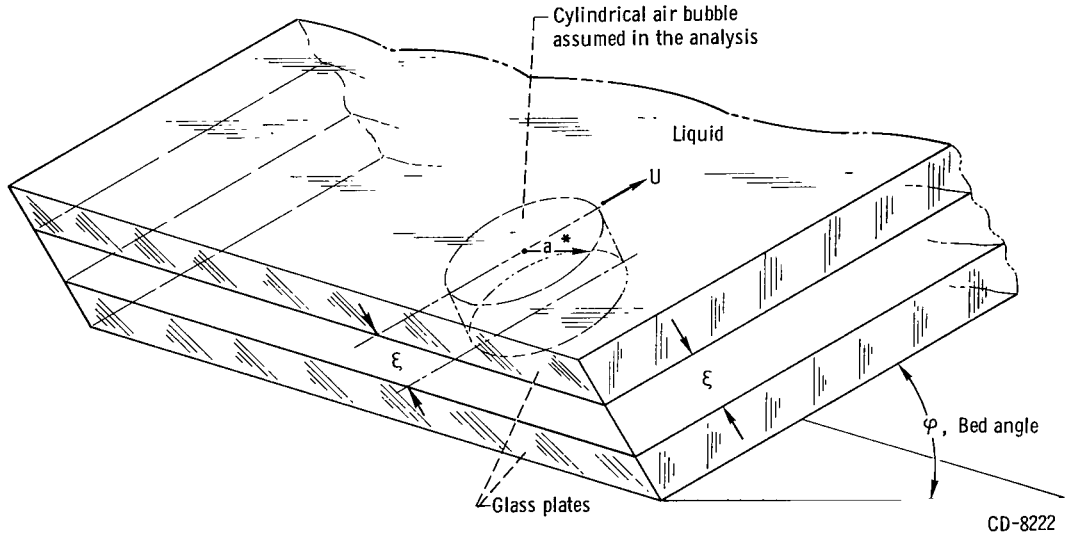

Figure 17. - Bed angle measurement by bubble movement.

"The aeronautical and space activities of the United States shall be conducted so as to contribute . . . to the expansion of human knowledge of phenomena in the atmosphere and space. The Administration shall provide for the widest practicable and appropriate dissemination of information concerning its activities and the results thereof."

—NATIONAL AERONAUTICS AND SPACE ACT OF 1958

NASA SCIENTIFIC AND TECHNICAL PUBLICATIONS

TECHNICAL REPORTS: Scientific and technical information considered important, complete, and a lasting contribution to existing knowledge.

TECHNICAL NOTES: Information less broad in scope but nevertheless of importance as a contribution to existing knowledge.

TECHNICAL MEMORANDUMS: Information receiving limited distribution because of preliminary data, security classification, or other reasons.

CONTRACTOR REPORTS: Technical information generated in connection with a NASA contract or grant and released under NASA auspices.

TECHNICAL TRANSLATIONS: Information published in a foreign language considered to merit NASA distribution in English.

TECHNICAL REPRINTS: Information derived from NASA activities and initially published in the form of journal articles.

SPECIAL PUBLICATIONS: Information derived from or of value to NASA activities but not necessarily reporting the results of individual NASA-programmed scientific efforts. Publications include conference proceedings, monographs, data compilations, handbooks, sourcebooks, and special bibliographies.

Details on the availability of these publications may be obtained from:

SCIENTIFIC AND TECHNICAL INFORMATION DIVISION

NATIONAL AERONAUTICS AND SPACE ADMINISTRATION

Washington, D.C. 20546